Theory of Steady-State Burning of Gas-Permeable Propellants

K. K. KUO*
The Pennsylvania State University, University Park, Pa.
AND
M. SUMMERFIELD†
Princeton University, Princeton, N.J.

High-speed flame propagation well above the normal deflagration rate can be achieved in the burning of porous propellants. Gas-penetrative burning of porous propellants under strong confinement is inherently self-accelerating. However, under suitable physical conditions, a constant-speed combustion wave can be produced. The jump conditions and the equivalent Rankine-Hugoniot relation for porous propellant burning are derived. An important result is that, whereas the usual R-H relation forbids the existence of a steady-state combustion wave that has both a pressure rise and a density decrease (called forbidden region on the R-H curve), this restriction can be bypassed in the situation discussed here, and high-speed compressive-expansive waves are legitimate solutions of the equations. It is shown also that the structure of the wave and its speed of propagation are affected by propellant porosity, ignition temperature, specific burning area, gas permeability and pressure. The flame propagation speed is determined as the eigenvalue of this two-point boundary value problem.

Nomenclature

a = pre-exponential factor for burning rate law
A_s = specific surface area, the surface exposed to fluid per unit spatial volume.
c_c = specific heat of the condensed phase
c_p = specific heat at constant pressure
D = drag force acting on gases by the pellets per unit wetted area of pellets
E = total stored energy per unit mass, $e+u^2/2$
F_o = force acting on the porous propellant grain at the cold end
h_c = the average heat-transfer coefficient over pellets
h_f = enthalpy of gas at adiabatic flame temperature
k = thermal conductivity of gases
k_p = thermal conductivity of pellets
n = exponent for the burning rate law
$\tilde{n}$ = number density of spherical pellets in the packed bed
P = pressure
Pr = Prandtl number
q_{ch} = chemical energy of the solid propellant
r_b = burning rate of the solid propellant
r_p = radius of pellets
R = gas constant
Re = Reynolds number
t = time
T = temperature
T_{abl} = ablation temperature of the solid propellant
T_f = adiabatic flame temperature of pellets
T_{ign} = ignition temperature of the solid propellant
T_{ps} = temperature of the pellet surface
T_o = initial temperature of pellets
u = gas velocity
v = gas velocity relative to the wave front
V = combustion wave propagation velocity
V_s = superficial gas velocity based on unobstructed flow area, $V_s = \phi u$
x = distance from the initial end surface of the porous propellant charge
α = thermal diffusivity
γ = specific heat ratio
δ_c = thickness of the preheat region
δ_i = location of the ignition plane
δ_t = total thickness of the combustion wave
ε_H = turbulent eddy diffusivity of heat
μ = gas viscosity
ξ = distance measured from the cold end of a stationary combustion wave in the porous propellant; it is defined in Eq. (7)
ρ = gas density
ρ_p = density of pellets
τ = new time coordinate defined by Eq. (7)
τ_{xx} = shear stress in the normal direction
ϕ = fractional porosity = $[1-\frac{4}{3}\pi r_p{}^3\tilde{n}]$
ψ = a function of distance defined by Eq. (12)

Subscripts

a = apparent
p = based upon pellet diameter or signifying pellets
o = cold end condition
∞ = hot end condition

Presented as Paper 73-221 at the AIAA 11th Aerospace Sciences Meeting, Washington, D.C., January 10–12, 1973; submitted February 16, 1973; revision received August 15, 1973. This paper represents the results of one part of the research work performed under Contract N00014-67-A-0151-0023 at Princeton University, under the supervision of the Power Branch of the Office of Naval Research. The work of the first author was continued after he joined Pennsylvania State University; this support is gratefully acknowledged.

Index categories: Combustion in Heterogeneous Media; Combustion Stability, Ignition, and Detonation.

* Assistant Professor, Department of Mechanical Engineering. Member AIAA.

† Professor of Aerospace Propulsion, Department of Aerospace and Mechanical Sciences. Fellow AIAA.

I. Introduction

THE burning rates of conventional high-energy solid propellants are usually limited by the thermal energy feedback to the regressing solid surface. The normal detonation wave speed of solid explosives or propellants is about 100,000 times higher than the speed of deflagration. A large part of the broad intermediate range of steady-state speeds between normal deflagration and detonation, which could be very useful for various practical applications, is actually forbidden by the Rankine-Hugoniot relations for conventional propellants. Nevertheless, the usual theories do not take into account the case of using unconventional propellants or unconventional means of energy feedback. Finding a mechanism for entering this forbidden range with a constant-velocity wave is the main objective of this paper. The burning of porous propellants offers

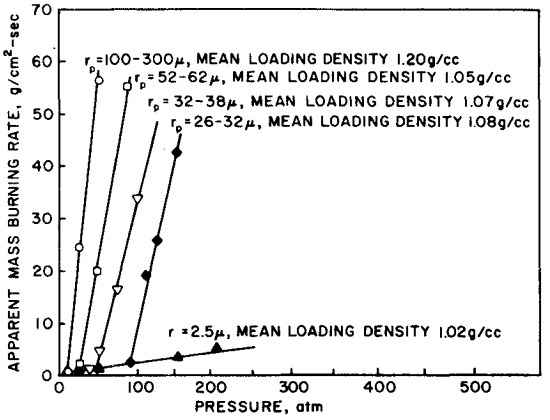

Fig. 1 Burning rates of pressed HMX powder at various pressures (measured by Taylor[6]).

the possibility of doing this. Unlike most of the previous investigations of the subject, which centered on hazards caused by the fast burning of porous propellant grains,[1-10] the current work emphasizes the practical use of a porous propellant as the main combustible substance in obtaining high gasification rates.

It is known from past experience and from previously published results[11-15] that gas-penetrative burning of porous propellants or explosives under strong confinement is inherently self-accelerating. However, under suitable physical conditions, where the driving pressure is constant and where the internal porous propellant structure and chemical properties are all properly selected, the internal pressure distribution generated by propellant gasification can produce a constant rate of gas penetration through the unburned portion, and may eventually give a constant speed of combustion-wave propagation. Experimentally, some evidence of steady gas-penetrative burning in porous propellants has been observed by several investigators.[1,6,8]

According to Taylor,[6] remarkably rapid rates of burning of PETN, RDX and HMX powders have been observed to occur above a transition pressure, the value of which varies with the explosive material, particle size, and loading density of the powder. The measured mass burning rate for various particle sizes of HMX powder is shown as a function of pressure in Fig. 1.

The transition from slow burning to rapid burning occurs at a low-pressure level when large particle sizes are used. This is due to the fact that large particles form large hydraulic pores, and hence the permeability of the explosive-powder charge is high. The transition from normal conductive burning into gas-penetrative convective burning is thus achieved at low pressures. Experimental results similar to those shown in Fig. 1 have also been measured by a number of investigators[1,8,16] for different propellants and explosives. Taylor also showed that he was able to change the speed of flame propagation by changing the conditions at the unburned end of the charge. He observed relatively constant speeds of flame propagation along a major portion of the powder charge.

A regime of stationary convective burning having a rate substantially above the normal burning rate has also been observed by Andreev and Chuiko.[1] For example, they found that combustion of low-density PETN at high pressures can proceed in a stationary manner at a rate several tens of time greater than the normal conductive burning rate.

Whether these observed results truly indicate stationary gas-penetrative burning is a question yet to be verified by burning extremely long charges of propellant under constant external pressure. Although these observations of stationary propagation may not prove the existence of a true steady state, they nevertheless indicate that the temporal change in the combustion wave is not very significant during the period of observed constant-speed propagation. (Some further discussion concerning this point is given in the section of Discussion of Results.) The theoretical study of the steady-state propagating wave is therefore an interesting problem.

Experimental attempts in the past to utilize high-speed porous-propellant burning were seldom successful, but this was due, we believe, to the lack of a theoretical framework for guiding the grain-development work and combustion experiments. The purpose of this theoretical investigation is to stimulate some decisive experiments and also to establish some useful guidelines for future development work in achieving control of porous-propellant burning.

II. Analysis

1. Description of the Physical Model

Following our previous work on transient burning of porous propellants,[11,12] we consider a long adiabatic cylindrical tube packed with commercial double-based spherical pellets (Fig. 2). Although the theory we develop here is quite general, several specific features and specific dimensions are chosen in advance in order to proceed later with numerical calculations. The consideration of spherical pellet shape is convenient for this paper because of the ready availability of known empirical heat-transfer and pressure-drop correlations for flow through a packed bed of spheres. However, this does not imply that the model considered in the current analysis cannot be applied in handling irregularly shaped particles or a cast monolithic propellant with any shape of pores. The theoretical model to be discussed can readily be modified to consider other configurations as soon as the gas-permeability, heat-transfer coefficient, effective micro-web thickness and specific surface area of the charge are known.

The void portion of the packed bed is filled initially with an inert gas at any given pressure. The propellant and the gas in the voids are at a uniform temperature. The porous propellant bed is ignited at the left end either by a gaseous or electrical igniter. Immediately after ignition, a part of the reacted gases leaving the burning surfaces of the pellets starts to flow into the unburned portion. Along with the infiltration of the hot gas into the cold unburned portion, energy is transferred from the hot gas to the cold propellant. The rate of energy transfer by this convective mechanism depends upon the velocity of the gas through the porous medium and also on the local pressure. The higher the gas velocity and pressure, the higher the rate of heat transfer and the faster the speed of the ignition front.

As the ignition front moves to the right, the igniter is turned off and the pressure at the consumed end is regulated by a controllable vent nozzle to stay at a fixed value. After the starting transient, a stationary combustion wave is produced and propagates at a constant speed. From then on, the propellant bed regresses at this constant rate and the pressure at the consumed end is maintained at a constant level. It is vitally important to keep a constant pressure there, since the main cause of explosions in the combustion of porous charges is due to a continuous increase in pressure.[17]

The speed of the combustion wave depends strongly upon the pressure gradient across the wave, the gas-permeability of the

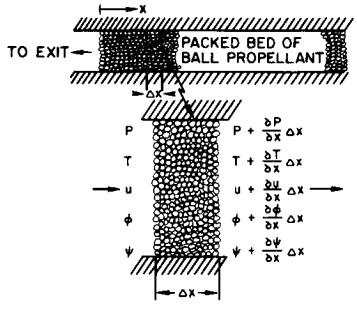

Fig. 2 Control volume considered in the analysis.

propellant charges, fractional porosity, ignition temperature of the propellant, and specific burning area. Conversely, the speed is the key parameter that governs the over-all wave structure and the location of the reacted state of the Hugoniot curve. The mathematical model developed in this analysis is mainly to determine the propagation velocity of the combustion wave, V, which is shown in the following to be the eigenvalue of this problem.

2. Basic Assumptions

It is important to point out here that the maximum pressure in the system is about two orders of magnitude lower than the detonation pressure of most solid explosives and propellants, which usually lies around 100 kbar. Since we are not dealing with extremely high pressures, the following assumptions are made to simplify the analysis involved.

a) A perfect gas law is used. This assumption must be abandoned if one extends the current analysis to the so-called LVD (low-velocity-detonation) region.

b) Propellant grains are considered to be fixed in space as in a firmly cemented propellant bed. We realize that under certain experimental conditions some fragments of the charge may be ejected rearward from the surface and burned in the gas stream. This phenomenon is actually observed[17] when the reacted gas has penetrated effectively into a perforated charge with very small pores; eruption is due to the reverse pressure gradient in the pores. The theory shows that this can occur.[11] However, when the porous propellant grain is made of a packed bed of propellant pellets or some granular explosive materials, the porosity is relatively large, and there are wide channels for the escape of gases, and so the local rise in pressure is less likely to cause eruptions.[17] In addition, the pellet sizes we considered are small; their lifetimes are short. Even though there is some motion in the reaction zone, this does not change the wave speed by a significant amount. The driving portion of the combustion wave is still governed mainly by the preheat region which describes the gas-penetrative motion ahead of the ignition front.

c) The flow of gas in the porous medium is considered to be one-dimensional. This assumption is commonly used in the study of the deflagration-to-detonation transition.[4,5]

3. Mathematical Model of the Steady-State Combustion Wave

To determine the detailed structure of the steady-state combustion wave, the governing partial differential equations for the gas phase developed in our previous analysis[11,12] for the transient burning of porous propellants are transformed into a system of ordinary differential equations. (The validity of the theoretical model for transient burning problems has been verified by very good agreement between theoretical predictions[11,12] and experimental results[13,14] in the burning of a packed bed of granular pellets in a closed chamber.) The governing equations for the transient case were deduced from the conservation equations for the gas phase; where the mass conservation equation is

$$\partial(\rho\phi)/\partial t+\partial(\rho\phi u)/\partial x = A_s\rho_p r_b \tag{1}$$

The momentum equation is

$$\frac{\partial(\rho\phi u)}{\partial t}+\frac{\partial(\rho\phi u^2)}{\partial x}=\frac{\partial(\phi\tau_{xx})}{\partial x}-A_s D-\phi\frac{\partial P}{\partial x} \tag{2}$$

and the energy equation is

$$\frac{\partial(\rho\phi E)}{\partial t}+\frac{\partial(\rho\phi uE)}{\partial x}=A_s\rho_p r_b h_f-h_c A_s(T-T_{ps})-\frac{\partial(\phi uP)}{\partial x}+\frac{\partial}{\partial x}\left[C_p\rho\phi(\alpha+\varepsilon_H)\frac{\partial T}{\partial x}\right]+\frac{\partial}{\partial x}[\phi u\tau_{xx}] \tag{3}$$

where $A_s = 3(1-\phi)/r_p$ for a packed bed of spheres.

After neglecting the work done by viscous stress and heat conduction term in the gas phase, and substituting the perfect gas law into the conservation equations, the following set of governing equations is obtained.

$$\frac{\partial T}{\partial t}+u\frac{\partial T}{\partial x}+(\gamma-1)T\frac{\partial u}{\partial x}=-\frac{(\gamma-1)Tu}{\phi}\frac{\partial\phi}{\partial x}-\frac{TA_s}{\phi P}(\gamma-1)h_c(T-T_{ps})+\frac{TA_s}{\phi P}\left\{\rho_p r_b\left(\gamma RT_f-RT+\frac{\gamma-1}{2}u^2\right)+(\gamma-1)uD\right\} \tag{4}$$

$$\frac{\partial P}{\partial t}+u\frac{\partial P}{\partial x}+\gamma P\frac{\partial u}{\partial x}=-\frac{(\gamma-1)A_s h_c(T-T_{ps})}{\phi}-\frac{\gamma Pu}{\phi}\frac{\partial\phi}{\partial x}+\frac{A_s}{\phi}\left\{r_b\left(\gamma\rho_p RT_f-P+\frac{\gamma-1}{2}\rho_p u^2\right)+(\gamma-1)uD\right\} \tag{5}$$

$$\frac{\partial u}{\partial t}+u\frac{\partial u}{\partial x}+\frac{1}{\rho}\frac{\partial P}{\partial x}=-\frac{A_s}{\phi\rho}\{r_b u\rho_p+D\} \tag{6}$$

In order to obtain the steady-state wave structure, the coordinate system is taken for convenience to travel at the same velocity as the combustion wave. Denoting the constant wave-propagation velocity by V and the new space coordinate by ξ, the transformation can be written as

$$\xi = Vt-x \qquad \tau = t \tag{7}$$

where τ is the new time coordinate. After transforming the governing partial differential equations (4–6) into the $\tau-\xi$ space and neglecting the time-derivative terms, and carrying out some algebraic manipulations, these ordinary differential equations are obtained. They are

$$\frac{dv}{d\xi}=\frac{A_s}{\phi P[1-(v^2/\gamma RT)]}\left\{r_b\left[\rho_p RT_f+P\left(\frac{\gamma-1}{\gamma}-\frac{v}{V}\right)\right]+\frac{r_b\rho_p(V-v)}{2\gamma}[(\gamma-1)V-(\gamma+1)v]+D\left[\frac{\gamma-1}{\gamma}V-v\right]-h_c\frac{\gamma-1}{\gamma}(T-T_{ps})\right\} \tag{8}$$

$$\frac{dT}{d\xi}=\frac{A_s T}{\phi P[1-(v^2/\gamma RT)]}\left\{\frac{(\gamma-1)}{\gamma}r_b\left[\frac{Pv^2}{RT}\left(\frac{1}{V}-\frac{1}{v}\right)+\frac{P}{v}+\left(1-\frac{v^2}{RT}\right)\frac{\rho_p}{2v}(V-v)^2\right]+r_b\rho_p\left[(V-v)+\frac{R(T_f-T)}{v}-v\frac{T_f}{T}-\frac{V-2v}{\gamma}\right]+\frac{\gamma-1}{\gamma}D\left[1+\left(1-\frac{v^2}{RT}\right)\left(\frac{V}{v}-1\right)\right]+h_c(\gamma-1)\frac{T-T_{ps}}{v}\left[\frac{v^2}{\gamma RT}-\frac{1}{\gamma}\right]\right\} \tag{9}$$

$$\frac{dP}{d\xi}=\frac{A_s}{\phi[1-(v^2/\gamma RT)]}\left\{-r_b\left[\rho_p v\left(1+\frac{T_f}{T}-\frac{V}{v}\right)+\frac{Pv}{RT}\left(1-\frac{1}{\gamma}-\frac{v}{V}\right)\right]-r_b\frac{\gamma-1}{2}\frac{v}{\gamma RT}\rho_p(V-v)^2+D\left[1-(\gamma-1)\frac{v(V-v)}{\gamma RT}\right]+h_c(\gamma-1)(T-T_{ps})\frac{v}{\gamma RT}\right\} \tag{10}$$

where v is the flow velocity relative to the wave front, i.e., $v \equiv V-u$.

The change of porosity with ξ is solely due to the surface regression of pellets; hence we have

$$d\phi/d\xi = A_s r_b/V \tag{11}$$

The heat conduction equation for the solid phase is reduced to an ordinary differential equation by an integral method similar to that used in our previous transient analysis.[11] The pellet surface temperature, T_{ps}, is related to the spatial-dependent function ψ by the following equation:

$$T_{ps}(\xi) = T_o[e^{\psi(\xi)}-\psi(\xi)] \tag{12}$$

The change of ψ with respect to ξ deduced from the integral method is

$$\frac{d\psi}{d\xi}=\frac{\alpha_p}{Vr_p^2}\frac{e^{\psi}-\psi-1+\frac{r_p h_c}{k_p}\left[\frac{T}{T_o}-e^{\psi}+\psi\right]}{e^{\psi}\left[\frac{1}{\psi}-\frac{2}{\psi^2}+\frac{2}{\psi^3}\right]-\frac{2}{\psi^3}-\frac{1}{3}} \tag{13}$$

The five ordinary differential equations (8–11, and 13) form a complete set describing the shape of the steady-state combustion wave propagated by the convective mechanism of energy transfer. This system of equations can be reduced further to four ordinary differential equations and one algebraic equation which is the integrated continuity equation from 0 to ξ

$$\rho_o V\phi_o+\rho_p V(1-\phi_o)=\rho v\phi+\rho_p V(1-\phi) \tag{14}$$

where the subscript o designates the conditions at the unburned end of the wave. This integrated continuity equation is used to replace any one of the four differential equations (8–11).

In principle, the integrated momentum and energy equations can also be used to replace two other differential equations among these four equations. However, the integrated momentum and energy equations for the porous propellant, unlike the conventional jump conditions, are not in simple algebraic form. Denoting the hot end conditions by the subscript ∞, the integrated continuity equation becomes

$$\rho_o V\phi_o+\rho_p V(1-\phi_o)=\rho_\infty v_\infty \tag{15}$$

The integrated momentum equation becomes

$$P_o\phi_o+\rho_o V^2\phi_o+\int_o^\infty A_s D\,d\xi+\int_o^\infty P\left(\frac{d\phi}{d\xi}\right)d\xi=P_\infty+\rho_\infty v_\infty{}^2 \tag{16}$$

and the integrated energy equation is

$$\rho_o V\phi_o\left(c_p T_o+\frac{V^2}{2}\right)+\rho_p V(1-\phi_o)\left(c_c T_o+\frac{V^2}{2}+q_{ch}\right)+V\left[\int_o^\infty A_s D\,d\xi+\int_o^\infty P\left(\frac{d\phi}{d\xi}\right)d\xi-(1-\phi_o)\rho_p V^2\right]=\rho_\infty v_\infty\left(c_p T_\infty+\frac{v_\infty{}^2}{2}\right) \tag{17}$$

The integral terms in Eqs. (16) and (17) are unusual; they come from the thrust of the solid-propellant bed. Thus, due to the presence of these integral terms in the momentum and energy jump equations, they cannot be used for replacing other ordinary differential equations in the original set. These thrust terms are very important. They are discussed again in Sec. 5 with respect to their role in modifying the R-H relation so as to permit the existence of steady-state solutions within the usual forbidden range.

To describe the structure of this stationary flame, it is convenient to divide the combustion wave into three distinct regions (see Fig. 3): a preheat region from $\xi=0$ to δ_c, an ignition region from $\xi=\delta_c$ to δ_i, and a reaction region from δ_i to δ_t. The demarcation between the preheat and ignition regions is defined by the specified ablation temperature of the propellant, and the demarcation between the ignition and reaction regions is defined by the specified ignition temperature of the solid propellant. The total thickness of the combustion wave, δ_t, is determined by the position where all the solid propellant is consumed, i.e., $\phi=1$.

In the preheat region, the condensed phase is heated up to the ablation temperature, hence the burning rate r_b is zero and the porosity is constant $\phi=\phi_o$. The equations governing the wave shape in this region are three ordinary differential equations (9, 10 and 13) and one algebraic relation, that is $\rho v=\rho_o V$. The boundary conditions at $\xi=0$ are

$$T(0)=T_o, \qquad P(0)=P_o, \qquad \psi(0)=\varepsilon \tag{18}$$

where ε is any small number other than zero. The reason for using ε to replace zero is to avoid the isolated singularity at $\xi=0$. It is found that the solution is not sensitive to the value of ε.

In addition to these fundamental equations and boundary conditions, one needs particular expressions for the drag per unit wetted area of pellets (D) and the heat-transfer coefficient (h_c) in order to proceed with the calculation on a computer. The expression for D, deduced from Ergun's equations[18] for the pressure drop correlation in a nonfluidized packed bed of spheres, is

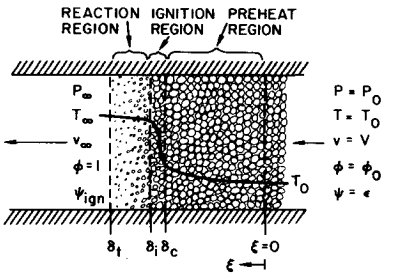

Fig. 3 Structure of a stationary combustion wave.

$$D=\frac{\rho(V-v)|V-v|}{6\phi}\left[150\frac{1-\phi}{Re_p}+1.75\right] \tag{19}$$

where Re_p designates the Reynolds number based upon the diameter of pellets and the superficial velocity V_s. (V_s is the average linear velocity of the fluid in the cylindrical chamber if no obstruction were present. The equation $V_s=\phi u$ is known as the Dupuit-Forchheimer relation.) The Reynolds number Re_p can therefore be written as $Re_p=\phi|V-v|\rho d_p/\mu$. The heat-transfer coefficient deduced from Denton's correlation[19,20] is

$$h_c=0.65\frac{k}{r_p}\left[\frac{\rho|V-v|\phi r_p}{\mu}\right]^{0.7}Pr^{1/3} \tag{20}$$

The third empirical correlation required is the regression rate of the propellant. A simple propellant burning-rate law

$$r_b=aP^n \tag{21}$$

is used for burning pellets.

With an estimated value of V, the computation can be performed from $\xi=0$ to δ_c, where the calculated ψ reaches ψ_{abl}, which is related to the given ablation temperature of the solid, T_{abl}, through Eq. (12).

In the ignition region, the integrated continuity equation (14) is used together with four ordinary differential equations, given by Eqs. (9–11, and 13), to determine the wave shape. The four boundary conditions at δ_c are

$$\left.\begin{aligned} &T(\delta_c)\\ &P(\delta_c)\end{aligned}\right\}\ \text{known from the preheat region calculation}$$
$$\left.\begin{aligned} &\psi(\delta_c)=\psi_{abl}\\ &\phi(\delta_c)=\phi_o\end{aligned}\right\} \tag{22}$$

The computation for this region is complete when ψ reaches ψ_{ign} corresponding to T_{ign}. This condition of full ignition also determines the position of δ_i. The burning rate, $r_b(\xi)$ in the ignition region rises from a value of zero to the fully-ignited burning rate represented by Eq. (21). The heat-transfer coefficient $h_c(\xi)$ acts just in the opposite manner. It decreases from its value at the ablation front to nearly zero at the plane of ignition. Since the ignition region is usually very narrow, the wave shape in this region is not affected by any significant amount by using different ramp functions.

In the reaction region, the propellant surface temperature can be considered constant. To simplify matters, we take this burning surface temperature equal to the ignition temperature, i.e., $T_{ps}(\xi\geq\delta_i)=T_{ign}$. The heat transfer between the gas- and solid-phases is then taken as zero. In addition to the mass continuity equation (14) in the algebraic form, the three simultaneous ordinary differential equations for determining the wave shape are Eqs. (9–11). The three boundary conditions at δ_i are the calculated values of T, P and ϕ at the end of the ignition region. The two boundary conditions at the consumed end of the reaction region are

$$P(\delta_t)=P_\infty \tag{23}$$

$$\phi(\delta_t)=1 \tag{24}$$

These two extra boundary conditions are used for determining the two characteristic unknowns of the problem: the wave propagation velocity (V) and the wave thickness (δ_t). A steady-state wave profile is considered solved when the solution, based

upon the assumed value of V, satisfies all the boundary conditions at both ends of the wave.

Across the whole combustion wave, the complete domain of interest can be regarded as governed by four differential equations, Eqs. (9–11, and 13), and one algebraic relation, Eq. (14). There are in total six boundary conditions: four at the cold end [three conditions specified by Eq. (18) plus $\phi(0) = \phi_o$] and two at the hot end [Eqs. (23) and (24)]. The two extra boundary conditions are used for determining V and δ_t.

4. Uniqueness of the Theoretical Solution

One may raise the question about the uniqueness of the solution since there are two characteristic values to be determined. To answer this question, the independent variable ξ in the reaction zone can be replaced by the new independent variable ϕ. This is achieved by dividing Eqs. (9) and (10) by Eq. (11). As a result, the number of differential equations for the reaction region is reduced from three to two. The boundary conditions for the reaction region using ϕ as the independent variable become

$$\left.\begin{array}{l} T(\phi_i) \\ P(\phi_i) \end{array}\right\} \text{ known from the ignition region calculation} \qquad P(1) = P_\infty \tag{25}$$

where ϕ_i is the porosity at the end of the ignition region. Here we have two ordinary differential equations but three boundary conditions; this extra boundary condition determines the eigenvalue V. This procedure essentially eliminates the introduction of the total wave thickness, δ_t, in solving the problem. δ_t can always be obtained by integrating Eq. (11) after the solution for the eigenvalue V and the wave shape as a function of ϕ have been determined. This indicates that although V and δ_t are both unknowns in this problem, V is the substantial eigenvalue of the problem. Therefore, the solution must be unique.

5. The Equivalent Rankine-Hugoniot Relation for Porous-Propellant Burning

The jump conditions across a combustion wave in a porous propellant were given by Eqs. (15–17). They are the integrated continuity, momentum, and energy equations. With a given equation of state of the gas at the fully reacted end, one would think that it is possible to deduce from these four equations a single equation relating only the pressure and density of the gas at the totally consumed end. That relation is usually called the Rankine-Hugoniot relation. However, when the jump conditions involve complicated integral terms, the situation is different. There is no single equation which relates the pressure and density at the hot burned end.

To simplify the forms of the integrated momentum and energy equations, one could use the momentum balance in the solid phase which is

$$\frac{F_o}{A} = \int_o^\infty A_s D\, d\xi + \int_o^\infty P\left(\frac{d\phi}{d\xi}\right) d\xi - (1-\phi_o)\rho_p V^2 \tag{26}$$

where F_o is the force acting on the porous propellant charge at the cold end. After substituting Eq. (26) into Eq. (16), the over-all integrated momentum equation becomes

$$[P_o\phi_o + \rho_o V^2\phi_o] + [(F_o/A) + \rho_p V^2(1-\phi_o)] = P_\infty + \rho_\infty v_\infty{}^2 \tag{27}$$

which says that the sum of the stream thrust of the gas and solid phases at the cold end is equal to the stream thrust of the gas at the burned end.

By substituting Eq. (26) into Eq. (17), the over-all integrated energy equation becomes

$$\rho_o V\phi_o\left(c_p T_o + \frac{V^2}{2}\right) + \rho_p V(1-\phi_o)\left(c_c T_o + \frac{V^2}{2} + q_{ch}\right) + \frac{F_o V}{A} = \rho_\infty v_\infty\left(c_p T_\infty + \frac{v_\infty{}^2}{2}\right) \tag{28}$$

which says that the total enthalpy (thermal, chemical and kinetic) of the gas and solid phases at the cold end plus the work input to keep the porous propellant burning at a fixed position is equal to the total enthalpy of the fully reacted gas.

To simplify the continuity equation, we can define an apparent density of the reactant as

$$\rho_a \equiv \rho_o\phi_o + \rho_p(1-\phi_o) \tag{29}$$

The continuity equation then becomes

$$\rho_a V = \rho_\infty v_\infty \tag{30}$$

Combining Eqs. (30) and (27), the equivalent Rayleigh line is obtained, namely

$$(\rho_\infty v_\infty)^2 = \frac{P_\infty - [P_o\phi_o + (F_o/A)]}{(1/\rho_a) - (1/\rho_\infty)} \tag{31}$$

Setting the specific heat of the gas equal to that of the solid, as in the usual discussion of the R-H relation, and combining Eqs. (27, 28, and 30) and the equation of state, an equivalent Rankine-Hugoniot relation for porous propellant combustion is obtained, that is

$$\frac{\gamma}{\gamma-1}\left(\frac{P_\infty}{\rho_\infty} - \frac{P_o}{\rho_o}\right) - \frac{1}{2}\left(P_\infty - P_o\phi_o - \frac{F_o}{A}\right)\left(\frac{1}{\rho_a} + \frac{1}{\rho_\infty}\right) = \frac{\rho_p(1-\phi_o)}{\rho_a} q_{ch} + \frac{F_o}{A\rho_a} \tag{32}$$

It is called an equivalent Rankine-Hugoniot relation because it is not a relationship between thermodynamic properties alone; the velocities of the gas and solid are still contained in F_o. The velocities have not been totally eliminated. However, this equation is still quite useful as soon as F_o is measured or estimated from some known combustion-wave structure.

For a fixed value of F_o, Eq. (32) relates P_∞ to ρ_∞; the nature of this equivalent R-H relation has been studied. It has been proved mathematically that all the conventional Rankine-Hugoniot properties[21] are preserved when a new origin based upon the apparent density, ρ_a, and apparent pressure, P_a, is used; and P_a is defined by

$$P_a \equiv P_o\phi_o + F_o/A \tag{33}$$

A Hugoniot curve for fixed values of F_o and q_{ch} is shown schematically in Fig. 4. The old origin, based upon the apparent (porous) propellant density and initial gas pressure, is also shown in the same figure. It is important to note that the new origin of the Hugoniot curve is shifted to a much higher pressure level due to the contribution of the thrust per unit area in the solid phase. It is shown clearly on this R-H diagram that the allowed region for real burning rates is thus significantly enlarged when a porous propellant is considered. This is what makes it possible to enter the "forbidden" speed range of the usual R-H diagram.

In most observed convective burning of porous charges, although a part of the reacted gas flows into the voids of the unburned portion to facilitate the flame propagation, the bulk flow of the reacted gas still moves away from the combustion wave. This means $v_\infty > V$. From the continuity equation (30), we have $1/\rho_\infty > 1/\rho_a$. This indicates that the convective burning

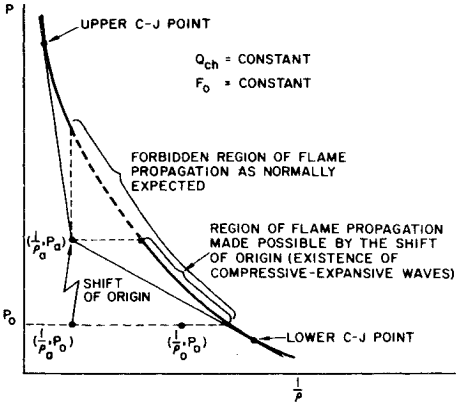

Fig. 4 Equivalent Rankine-Hugoniot curve.

Table 1 Data used in the numerical computations

ρ_p	$= 1.6$ gm/cm^3
α_p	$= 0.945 \times 10^{-3}$ cm^2/sec
k_p	$= 0.53 \times 10^{-3}$ cal/cm-sec-°K
T_{abl}	$= 450$°K
T_{ign}	$= 615$°K
T_f	$= 2860$°K
γ (500°K)	$= 1.4$
γ (3000°K)	$= 1.26$
k	$= 2.65 \times 10^{-4}$ cal/cm-sec-°K
μ	$= 0.223 \times 10^{-3}$ gm/cm-sec
T_o	$= 294.4$°K
P_o	$= 1033.23$ g/cm^2
r_b (cm/sec)	$= a[P(\text{kbar})]^n$
where	$a = 12.1$
	$n = 0.8867$

of porous propellant still belongs to the deflagration branch of the Hugoniot curve. This is the reason we employed in the Abstract the apparently contradictory term, compressive-expansive wave.

It is also important to point out that the equivalent R-H relation given by Eq. (32) can be applied to any porous charge configurations. The jump conditions [Eqs. (27, 28, and 30)] are also perfectly general.

III. Discussion of Results

The steady-state wave structure described by the theoretical model discussed in the analysis section can be computed in an iterative manner until the estimated value of the flame propagation speed, V, makes the corresponding combustion wave satisfy both boundary conditions simultaneously at the consumed end. However, a more economical method of computation can be used, which is to assign a value of V and to perform a direct integration from the cold to the hot end. The pressure at the fully-reacted end is determined from the computed gas pressure when the porosity reaches unity. By so doing, the iteration procedure is avoided.

A systematic numerical computation has been performed for a commercial double-based porous propellant. For the case of porosity equal to 0.377 and pellet radius of 100 μ four burning velocities [$V = 2500$, 3000, 3500 and 3800 cm/sec] are considered. Other data used in the numerical computations are shown in Table 1. A typical calculated combustion wave shape, which corresponds to $V = 3500$ cm/sec, is shown in Figs. 5a and 5b. The over-all wave thickness is about 5.5 cm which is quite thick in comparison with any conventional combustion waves,

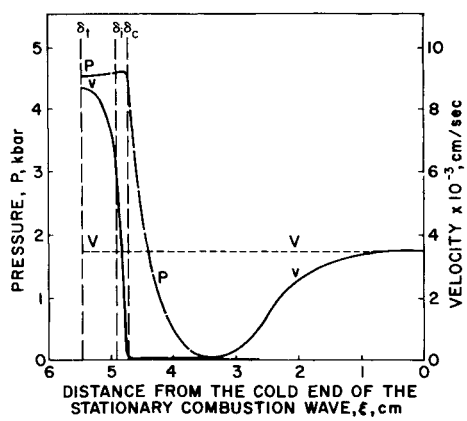

Fig. 5a Calculated distributions of pressure and velocities across the combustion wave in a porous propellant.

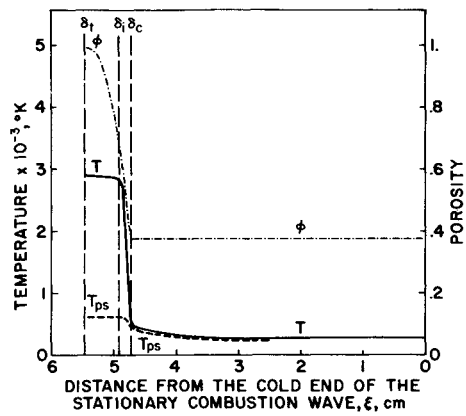

Fig. 5b Calculated distributions of porosity and temperatures across the combustion wave in a porous propellant.

including both premixed flames and diffusion flames. This is because in the high-porosity charge that we considered, the reacted gas can easily penetrate deeply into the highly permeable propellant. This kind of thick combustion wave has been observed by various investigators in porous-propellant or explosive studies.[1,5,6,17]

It is indicated in Figs. 5a and 5b that the major portion of the wave is the preheat region in which the velocities of the gas and of the solid phase start at some value at the cold unburned end relative to the flame. The solid phase maintains the constant speed V, which is the speed of regression of the porous charge, whereas the gas phase moves at a slower speed than V in the preheat region, and in this region the relative velocity increases in the ξ direction.

Because of the large area for heat transfer from the gas to the solid, the gas temperature is only slightly above the pellet surface temperature throughout the entire preheat region. Since no burning occurs in this region, the porosity remains constant.

The pressure of the gas in the voids of the preheat region starts with a very low value, P_o, at the cold end and rises sharply in the area near $\xi = \delta_c$. This pressure gradient gives the major driving potential to make the hot gas penetrate the unburned portion. The higher the pressure at δ_c the deeper the penetration of reacted gas into the voids.

In the ignition region, the gas temperature rises sharply due to the gasification of the solid phase; and the fractional porosity also increases there. The pressure in this region exhibits a small hump which causes the gas to flow partly into the preheat region and partly into the reaction region. The thickness of the ignition region depends upon the temperature difference between T_{ign} and T_{abl}. In the limit, when T_{ign} equals T_{abl}, the region disappears; it then becomes the bounding surface between the preheat and reaction regions.

The reaction region is also relatively thin in comparison with the preheat region. In this region, the porosity rises to unity at the totally consumed end. The pressure and temperature distributions are quite uniform, and the velocity of the gas increases to a value much higher than V.

The positions of the three regions as a function of P_∞ are shown on Fig. 6. As one would expect that at higher pressures the heat transfer is more efficient, therefore, δ_c decreases as P_∞ increases. Since the over-all combustion-wave thickness δ_t is governed mainly by δ_c, it also drops when P_∞ becomes higher. The calculated reaction zone becomes thicker when P_∞ is higher; this is due to the fact that the flame propagation speed is a sharply rising function of pressure. Because of the sharp increase of V with pressure, the reaction region spreads out as P_∞ increases. The actual lifetime of the pellets, from start of gasification to the fully-burned-out stage, is shorter at higher pressures.

The average slope of the calculated flame-propagation-velocity vs pressure shown in Fig. 6 is 5.9×10^3 (cm/sec)/kbar. Within

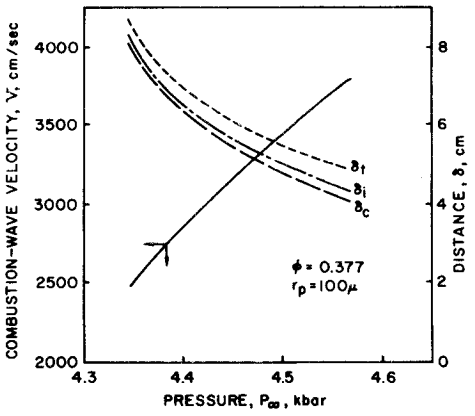

Fig. 6 Calculated effect of pressure on the combustion wave velocity and the positions of individual regions.

the pressure range studied, the velocity changes drastically with pressure: a 3% change of pressure makes a 20% change in velocity. It is interesting to note that steep relations of V vs P_∞ are observed in several published experimental works on the burning of porous charges. For example, the slopes (dV/dP_∞) measured by Taylor[6] for various particle sizes and loading densities (Fig. 1) range from 0.64×10^3 to 13.2×10^3 (cm/sec)/kbar, and the measured values of slopes by Bobolev[8] range from 1.9×10^3 to 10.7×10^3 (cm/sec)/kbar. These experimental results, however, correspond to a much lower level of pressure and velocity than that considered in this theoretical study; and so this coincidence of slopes cannot be taken immediately as confirmation of the theory. In fact, in the authors' opinion, a more complete picture of the combustion wave velocity, V, vs pressure should look like that shown on Fig. 7. In the low-pressure region, the convective burning observed by Taylor,[6] Bobolev,[8] and others may or may not be truly at steady state. Since the local thickness of the flame may not be small in comparison with the void space in the porous propellant or explosives, the combustion wave may not yet be fully developed into a stable and steady-state combustion wave. This could explain why unstable, oscillating flames have often been observed in the early stage of convective burning.

At an intermediate pressure, the growth of V with respect to P may not be linear, depending upon the geometrical configurations and combustion characteristics of porous charges. Some shapes similar to that shown schematically on Fig. 7 have actually been measured by various investigators.[1,22,23] True steady-state convective burning must occur at a pressure high enough that the local flame thickness is negligible in comparison with the effective hydraulic pore diameter in a porous charge. Therefore,

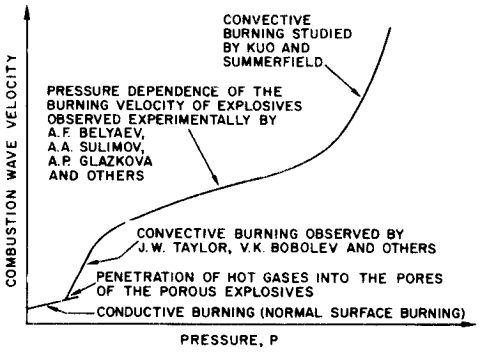

Fig. 7 Pressure dependence of the combustion wave velocity in porous propellants or explosives.

our steady-state solution lies at pressures much higher than those corresponding to the early phases of the convective burning.

Although a considerable amount of experimental data for gun systems has been taken at the high pressure ranges we studied (4 to 5 kbar), all the measurements, to these authors' knowledge, have been made under transient, and not steady-state, conditions. Since no systematic experimental data on the burning of porous charges in the range of pressure and permeability considered here are available, no direct comparison between theoretical results and experimental data can be made at this time.

IV. Conclusions

1) It is shown theoretically that high-speed steady-state combustion waves in porous propellants do exist. A theoretical model has been developed to describe the steady-state combustion-wave structure in gas-penetrative burning of a porous solid propellant. The flame speed has been shown to be the eigenvalue of a two-point boundary value problem. It is also shown analytically that the solution of this problem is unique.

2) The jump conditions and an equivalent Rankine-Hugoniot relation for a general porous-propellant combustion wave are derived. It is found that the origin of the equivalent Hugoniot curve is shifted to a much higher pressure level due to the contribution of the thrust per unit area in the solid phase. This shift of origin in the R-H diagram significantly enlarges the allowed region for real burning rates. This explains why it is possible to enter the "forbidden" speed range of the usual R-H diagram by using porous propellants.

3) It is proved mathematically that all the conventional R-H properties are preserved when the new origin, based upon the apparent pressure and apparent density, is used. For example, the Mach number of the product gas is unity at both upper and lower Chapman-Jouguet points. The entropy of the gas presents a maximum at the lower C-J point but reaches a minimum at the upper C-J point, etc.

4) It is shown that the generally observed gas-penetrative burning of a porous propellant lies on the deflagration branch of the equivalent R-H curve.

5) In order to obtain a steady-state or quasi-steady-state burning mode in a porous propellant, it is vitally important that the pressure at the reacted end be controlled.

References

[1] Andreev, K. K. and Chuiko, S. V., "Transition of the Burning of Explosives into an Explosion. I. Burning of Powdered Explosives at Constant High Pressures," *Russian Journal of Physical Chemistry*, Vol. 37, No. 6, 1963, pp. 695–699.

[2] Andreev, K. K., "On the Transition to Explosion of the Burning of Explosives," *Journal of Combustion and Flame*, Vol. 7, June 1963, pp. 175–183.

[3] Belyaev, A. F., Sukoyan, M. K., Korotkov, A. I., and Sulimov, A. A., "Consequences of the Penetration of Combustion into an Individual Pore," translated from *Fizika Goreniya i Vzryva*, Vol. 6, No. 2, April–June 1970, pp. 166–171.

[4] Aleksandrov, E. N., Veretennikov, V. A., Dremin, A. N., and Shvedov, K. K., "The Detonation Mechanism in Porous Explosives," translated from *Fizika Goreniya i Vzryva*, Vol. 3, No. 4, Oct.–Dec. 1967, pp. 471–484.

[5] Griffiths, B. N. and Groocock, J. M., "The Burning to Detonation of Solid Explosives," *Journal of the Chemical Society*, Vol. 814, 1960, p. 4154.

[6] Taylor, J. W., "The Burning of Secondary Explosive Powders by a Convective Mechanism," *The Faraday Society*, Vol. 58, No. 471, 1962, pp. 561–568.

[7] Bernecker, R. R. and Price, D., "Transition from Deflagration to Detonation in Granular Explosives," NOLTR 72-202, Dec. 1972, Naval Ordnance Lab., White Oak, Silver Spring, Md.

[8] Bobolev, V. K., Margolin, A. D., and Chuiko, S. V., "Stability of Normal Burning of Porous Systems at Constant Pressure," Translated from *Fizika Goreniya i Vzryva*, Vol. 2, No. 4, 1966, pp. 24–32.

[9] Godai, T., "Flame Propagation into the Crack of Solid Propellant Grain," TR-91, 1965, National Aerospace Lab., Tokyo, Japan; also *AIAA Journal*, Vol. 8, No. 7, July 1970, pp. 1322–1327.

[10] Korotkov, A. I., Sulimov, A. A., Obmenin, A. V., Dubovitskii, V. F., and Kurkin, A. I., "Transition of Burning to Detonation in Porous Explosives," Translated from *Fizika Goreniya i Vzryva*, Vol. 5, No. 3, 1969, p. 315.

[11] Kuo, K. K., Vichnevetsky, R., and Summerfield, M., "Theory of Flame Front Propagation in Porous Propellant Charges under Confinement," *AIAA Journal*, Vol. 11, No. 4, April 1973, pp. 444–451.

[12] Kuo, K. K., Vichnevetsky, R., and Summerfield, M., "Generation of an Accelerated Flame Front in a Porous Propellant," AIAA Paper 71-210, New York, 1971.

[13] Squire, W. H. and Devine, M. P., "The Interface Between Primer and Propellant," Pt. I and Pt. II, AOA Paper, 1969, Frankford Arsenal, Philadelphia, Pa.

[14] Squire, W. H., private communication, 1970–1971, Frankford Arsenal, Philadelphia, Pa.

[15] Kitchens, C. W., Jr., "Flame Spreading in Small Arms Ball Propellant," Rept. 1604, Aug. 1972, Ballistic Research Labs., Aberdeen Proving Ground, Md.

[16] Kondrikov, B. N. and Ma, C. Y., "The Effect of Pressure and Temperature on the Burning of Powdery Explosive Materials in Low Density Charges," *The Theory of Explosive Materials*, Moscow, 1967, pp. 207–221.

[17] Bobolev, V. K., Karpukhin, I. A., and Chuiko, S. V., "Combustion of Porous Charges," *Journal of Combustion, Explosion and Shock Waves*, Vol. 1, No. 4, 1966, pp. 31–36.

[18] Bird, R. B., Stewart, W. E., and Lightfoot, E. N., *Transport Phenomena*, Wiley, New York, 1960, pp. 180–200.

[19] Eckert, E. R. G. and Drake, R. M., Jr., *Heat and Mass Transfer*, McGraw-Hill, New York, 1959, pp. 248–253.

[20] Soo, S. L., *Fluid Dynamics of Multiphase Systems*, Blaisdell, Waltham, Mass., 1967, Chap. 6, pp. 248–276.

[21] Williams, F. A., *Combustion Theory*, Addison-Wesley, Reading, Mass., 1965, Chap. 2.

[22] Glazkova, A. P. and Tereshkin, I. A., "Pressure Dependence of the Burning Velocity of Explosives," *Russian Journal of Physical Chemistry*, Vol. 35, No. 7, July 1961, pp. 795–800.

[23] Belyaev, A. F., Korotkov, A. I., Parfenov, A. K., and Sulimov, A. A., "Burning Velocities of Explosives under Very High Pressures," *Russian Journal of Physical Chemistry*, Vol. 37, No. 1, Jan. 1963, pp. 70–74.

JANUARY 1974 AIAA JOURNAL VOL. 12, NO. 1

Turbojet Exhaust Reactions in Stratospheric Flight

L. B. ANDERSON* AND J. W. MEYER†
Lockheed Palo Alto Research Laboratory, Palo Alto, Calif.
AND
W. J. MCLEAN‡
Cornell University, Ithaca, N.Y.

This paper summarizes computational results from chemical modeling of hot turbojet exhaust reactions under high-altitude flight conditions. Interest is in the near-field chemical fate of potential stratospheric pollutants in aircraft wakes. It is found that oxidation and reduction rates of carbon, nitrogen and sulfur species are controlled by super-equilibrium concentrations of radicals. Where there is complete afterburner oxidation of all hydrocarbons, H, O and OH radicals control the nozzle and exhaust jet core reactions. Under these conditions all NO_x is present as nitric oxide. However, if high levels of unburned hydrocarbons are present at the exhaust nozzle throat, HO_2, OH, and organic molecules are the dominant radical species. In this case there is appreciable production of H_2O_2 and NO_2 in the exhaust. Thus, under certain operating conditions, some NO_x may be converted to nitric acid in an aircraft wake. This process is expected to depend on exhaust composition and on cooling and dilution rates in the wake.

I. Introduction

ENVIRONMENTAL effects of high-altitude aircraft are of mounting interest as the number of flights at stratospheric altitudes increases. Emissions at high altitudes are particularly important because of the relatively long species residence times in the stratosphere. Concern has been expressed over the effect of emissions on the stratospheric ozone layer shielding the Earth from ultraviolet radiation, and catalytic destruction of ozone by nitrogen oxide (NO_x) emissions may be an important consideration in high-altitude aircraft operations.

For any systematic attempt to evaluate the ultimate environmental impact of exhaust emissions in stratospheric flight, a knowledge of the amounts of potentially important species which are deposited in the stratosphere is needed. Experimental measurements made in the hot exhaust gas near the exit regions of representative aircraft engines may not provide this information for at least two reasons. First, some potentially important species may be inaccessible to quantitative measurement techniques under these conditions. Second, chemical reactions in the exhaust may destroy or give rise to potentially important species downstream from the exit plane of the engine.

The objective of the present study is to determine the nature and extent of those chemical reactions in the near-field flow which can alter the composition of environmentally significant species as the exhaust gases expand and cool to ambient

Presented as Paper 73-99 at the AIAA 11th Aerospace Sciences Meeting, Washington, D.C., January 10–12, 1973; submitted February 23, 1973; revision received August 27, 1973. This work has been supported by the Climatic Impact Assessment Program Office of the Secretary, U.S. Department of Transportation.

Index categories: Reactive Flows; Combustion in Gases; Thermochemistry and Chemical Kinetics.

* Manager, Chemistry Laboratory. Associate Fellow AIAA.

† Associate Research Scientist. Associate Member AIAA.

‡ Assistant Professor, Sibley School of Mechanical and Aerospace Engineering.